Time-Asynchronous Robust Cooperative Transmission for the Downlink of C-RAN

Seok-Hwan Park, *Member, IEEE*, Osvaldo Simeone, *Fellow, IEEE*, and Shlomo Shamai (Shitz), *Fellow, IEEE*

***Abstract*—This letter studies the robust design of downlink precoding for cloud radio access network (C-RAN) in the presence of asynchronism among remote radio heads (RRHs). Specifically, a C-RAN downlink system is considered in which nonideal fronthaul links connecting two RRHs to a baseband unit (BBU) may cause a time offset, as well as a phase offset, between the transmissions of the two RRHs. The offsets are *a priori* not known to the BBU. With the aim of counteracting the unknown time offset, a robust precoding scheme is considered that is based on the idea of correlating the signal transmitted by one RRH with a number of delayed versions of the signal transmitted by the other RRH. For this transmission strategy, the problem of maximizing the worst-case minimum rate is tackled while satisfying per-RRH transmit power constraints. Numerical results are reported that verify the advantages of the proposed robust scheme as compared to the conventional nonrobust design criteria as well as noncooperative transmission.**

***Index Terms*—Asynchronous transmission, cloud radio access network (C-RAN), fronthaul latency, robust optimization.**

I. Introduction

CLOUD radio access network (C-RAN) is a promising architecture to address the challenging requirements for the fifth generation (5G) of wireless communication systems in terms of reduced deployment costs, high data rate, and low power consumption [1]. In a C-RAN, a baseband processing unit (BBU) implements the baseband processing functionalities of a set of remote radio heads (RRHs) that are connected to the BBU by means of fronthaul links.

In order to realize these potential benefits of centralized processing at the BBU, it is necessary to deploy reliable and high-speed fronthaul links. Nevertheless, cost and technological limitations dictate the use of fronthauling technologies, such as wireless microwave or millimeter wave, that fall short of the ideal requirements of high capacity and perfect reliability. This has led researchers in both industry and academia to investigate the impact of fronthaul *capacity* constraints on the spectral efficiency, see, e.g., [2]–[4], as well as the effect of fronthaul *latency* on higher layer performance metrics [5] (see also review in [1]). This letter contributes to this line of work by studying the implications of, and countermeasures to, the imperfect mutual *synchronization* of the RRHs that may result from nonideal fronthaul connections to the cloud.

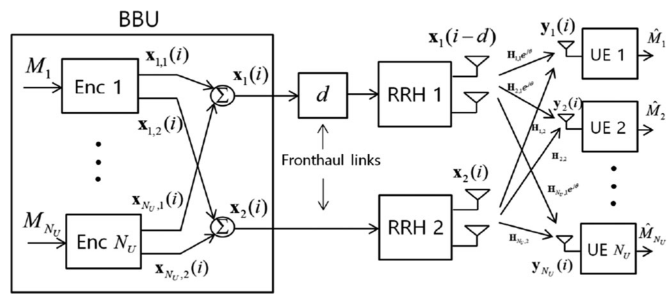

Fig. 1. Illustration of a C-RAN downlink with time offset.

To this end, we consider the C-RAN downlink system in Fig. 1 in which the transmission of the two RRHs is characterized by a relative time offset, as well as by a phase offset. These offsets are unknown to the BBU and are generally caused by imperfections in the transmission and processing of clock-bearing signals on the fronthaul links [6]. We specifically concentrate on the design of robust cooperative precoding strategies at the BBU across the two RRHs that account for the existing uncertainty regarding the inter-RRH time offset. The effect of the phase offset is also included in the model, but it is not the focus of the analysis of this letter.

The presence of an unknown time offset generally precludes the use of cooperative precoding across the two RRHs, since the RRHs only have radio frequency functionalities and cannot compensate for fronthaul inaccuracies. Owing to the time offset, the BBU cannot control the correlation of the signals transmitted by the RRHs, which, in turn, makes it impossible to ensure the constructive superposition of the RRHs' signals at the desired receivers. In fact, when the synchronization is imperfect, it may be beneficial to restrict transmission to noncooperative strategies, as studied in [7].

In this letter, we introduce and design a robust asynchronous cooperation scheme for C-RAN, which is motivated by the coding scheme proposed in [8] in the context of an asynchronous cognitive multiple access channel. In the considered setup, as detailed in Section II, the time offset is known by the BBU to lie in a bounded range. The main idea of the robust scheme, as discussed in Section III, is to correlate the signal to be transmitted by one RRH with different delayed versions of the signal to be transmitted by the other RRH. In this fashion, no matter what the actual time offset is, partial correlation between the transmitted signals can be preserved and, with it, cooperative gains can be potentially accrued. We note that, at a fundamental level, the idea can be thought of as a robust scheme for

Manuscript received June 27, 2016; accepted August 15, 2016. Date of publication August 17, 216; date of current version September 2, 2016. The work of S.-H. Park was supported by the National Research Foundation of Korea funded by the Korea Government (MSIP) under Grant NRF-2015R1C1A1A01051825. The work of O. Simeone was supported in part by U.S. NSF under Grant CCF-1525629. The work of S. Shamai has been supported by the European Union's Horizon 2020 Research And Innovation Programme under Grant 694630. The associate editor coordinating the review of this manuscript and approving it for publication was Prof. Francesco Verde.

S.-H. Park is with the Division of Electronic Engineering, Chonbuk National University, Jeonju-si 54896, Korea (e-mail: seokhwan@jbnu.ac.kr).

O. Simeone is with the Center for Wireless Communication and Signal Processing Research, New Jersey Institute of Technology, Newark, NJ 07102 USA (e-mail: osvaldo.simeone@njit.edu).

S. Shamai (Shitz) is with the Department of Electrical Engineering, Technion, Haifa 32000, Israel (e-mail: sshlomo@ee.technion.ac.il).

Color versions of one or more of the figures in this letter are available online at http://ieeexplore.ieee.org.

Digital Object Identifier 10.1109/LSP.2016.2601113

communication on a compound channel [9]. For this scheme, we tackle the problem of maximizing the worst-case minimum rate over the correlation matrices of the transmitted signals while satisfying the per-RRH power constraints in Section IV. Section V provides some numerical results that validate the advantages of the proposed robust scheme as compared to conventional cooperative and noncooperative strategies.

II. System Model

We consider the downlink of a C-RAN shown in Fig. 1, in which a BBU manages two RRHs that communicate with N_U user equipments (UEs). Specifically, by using its fronthaul connections to the RRHs, the BBU wishes to send a message $M_k \in \{1, \ldots, 2^{nR_k}\}$ to the kth UE, where R_k and n denote the rate of the message M_k and the coding block length, which is assumed to be sufficiently large to invoke information-theoretic arguments. We denote the numbers of the antennas of the jth RRH and the kth UE as $n_{R,j}$ and $n_{U,k}$, respectively, and define the sets $\mathcal{N}_U \triangleq \{1, \ldots, N_U\}$ and $\mathcal{N}_R \triangleq \{1, 2\}$ of the UEs and RRHs, respectively.

Unlike previous works that investigated the impact of fronthaul capacity or latency limitations (see, e.g., [1]), we study the impact of *asynchronism* among the two RRHs, which is caused by nonideal clock transfer or the fronthaul links. We model the lack of time synchronization with the baseline scenario in Fig. 1, in which RRH 1 has a time offset of d channel uses with respect to RRH 2, where the amount d is not known to the BBU. The BBU only knows that the delay d belongs to an uncertainty set $d \in \mathcal{D} = \{0, 1, \ldots, D\}$, where $D \geq 1$ represents the worst-case delay. As in standard C-RAN systems, the RRHs have only radio frequency functionalities and hence are not able to compensate for any asynchronism. No further fronthaul limitations, such as in terms of capacity, are accounted for in the model.

Under a flat fading channel model, the signal $\mathbf{y}_k(i) \in \mathbb{C}^{n_{U,k}\times 1}$ received by the kth UE on the ith channel use, $i \in \{1, \ldots, n\}$, is given as

$$\mathbf{y}_k(i) = \mathbf{H}_{k,1} e^{j\theta} \mathbf{x}_1(i-d) + \mathbf{H}_{k,2}\mathbf{x}_2(i) + \mathbf{z}_k(i) \tag{1}$$

where $\mathbf{x}_j(i) \in \mathbb{C}^{n_{R,j}\times 1}$ is the signal transmitted by the jth RRH during the ith channel use; $\mathbf{H}_{k,j} \in \mathbb{C}^{n_{U,k}\times n_{R,j}}$ is the channel matrix from the jth RRH to the kth UE; θ denotes the phase offset between the RRHs, which is also assumed to be unknown to the BBU; and $\mathbf{z}_k(i) \in \mathbb{C}^{n_{U,k}\times 1}$ is the additive noise vector distributed as $\mathbf{z}_k(i) \sim \mathcal{CN}(\mathbf{0}, \mathbf{I})$. We assume that the channel matrices $\{\mathbf{H}_{k,j}\}_{k\in\mathcal{N}_U, j\in\mathcal{N}_R}$, the time offset d and the phase offset θ remain constant during each coding block of n channel uses, and impose per-RRH transmit power constraints as $(1/n)\sum_{i=1}^{n} \|\mathbf{x}_j(i)\|^2 \leq P_j$.

As further detailed next, in this letter, we focus on the design of cooperative linear precoding with the aim of ensuring robustness with respect to the time asynchronicity $d \in \mathcal{D}$. The impact of the phase offset will be further studied in Section V via numerical results.

III. Asynchronous Robust Transmission

In this section, we describe the proposed asynchronous cooperative scheme for linear precoding across the two RRHs. The key idea of the proposed robust scheme is to make the signal $\mathbf{x}_2(i)$ transmitted by the RRH 2 correlated to both the current and the delayed versions $\{\mathbf{x}_1(i-d)\}_{d\in\mathcal{D}}$ of the transmit signal of RRH 1. This follows the idea proposed in [8], in which a general information-theoretic formulation was provided in the context of an asynchronous cognitive channel. The result was then applied in [8] to a system with *single-antenna* transceivers and a *single* user. As mentioned, the robust scheme is designed to counteract the unknown time offset d, but it assumes no phase offset, i.e., $\theta = 0$. Note that, from now on, we do not explicitly indicate the dependence of the signals on the channel use index to simplify the notation.

To elaborate, for any channel use, we define a vector $\bar{\mathbf{v}}_k = [\mathbf{v}_{k,0}^\dagger\, \mathbf{v}_{k,1}^\dagger \ldots \mathbf{v}_{k,D}^\dagger]^\dagger \in \mathbb{C}^{(D+1)n_{R,1}\times 1}$ for each UE $k \in \mathcal{N}_U$. This represents $D+1$ consecutive symbols from the precoded signal transmitted by RRH 1 and intended for UE k, with $\mathbf{v}_{k,i}$ being the signal sent when $d = i$. Superimposing the signals intended for different UEs, the signal $\mathbf{x}_1$ transmitted by RRH 1 when the delay is d is then given as

$$\mathbf{x}_1 = \sum_{k\in\mathcal{N}_U} \mathbf{v}_{k,d}. \tag{2}$$

The signal $\mathbf{x}_2$ transmitted by RRH 2 is also given as the superposition of the signals $\mathbf{x}_{2,k} \in \mathbb{C}^{n_{R,2}\times 1}$ intended for each UE k as

$$\mathbf{x}_2 = \sum_{k\in\mathcal{N}_U} \mathbf{x}_{2,k}. \tag{3}$$

Moreover, when the time offset is d, the received signal vector $\mathbf{y}_k$ of UE k, denoted as $\mathbf{y}_{k,d}$, is given as

$$\mathbf{y}_{k,d} = \mathbf{H}_{k,1} \sum_{l\in\mathcal{N}_U} \mathbf{v}_{l,d} + \mathbf{H}_{k,2} \sum_{l\in\mathcal{N}_U} \mathbf{x}_{2,l} + \mathbf{z}_k. \tag{4}$$

The key property of the robust precoding scheme is that the signal $\mathbf{x}_{k,2}$ transmitted by RRH 2 is correlated with the $D+1$ consecutive vectors $\mathbf{v}_{k,d}$, $d \in \mathcal{D}$, each of which is sent by RRH 1 when the delay is d. Specifically, the vectors $\bar{\mathbf{v}}_k$ and $\mathbf{x}_{k,2}$ are characterized by the covariance matrix

$$\mathbf{\Sigma}_{\mathbf{x}}(\mathbf{V}, \mathbf{\Sigma}_{\mathbf{x}_2}, \mathbf{\Omega}) = \mathbb{E}\left[\begin{bmatrix}\bar{\mathbf{v}}_k \\ \mathbf{x}_{2,k}\end{bmatrix}\begin{bmatrix}\bar{\mathbf{v}}_k^\dagger & \mathbf{x}_{2,k}^\dagger\end{bmatrix}\right] = \begin{bmatrix}\bar{\mathbf{V}}_k & \bar{\mathbf{\Omega}}_k \\ \bar{\mathbf{\Omega}}_k^\dagger & \mathbf{\Sigma}_{\mathbf{x}_{2,k}}\end{bmatrix} \tag{5}$$

where we defined the correlation matrices $\bar{\mathbf{V}}_k = \mathbb{E}[\bar{\mathbf{v}}_k \bar{\mathbf{v}}_k^\dagger]$, $\mathbf{\Sigma}_{\mathbf{x}_{2,k}} = \mathbb{E}[\mathbf{x}_{2,k}\mathbf{x}_{2,k}^\dagger]$ and $\mathbf{\Omega}_{k,d} = \mathbb{E}[\mathbf{v}_{k,d}\mathbf{x}_{2,k}^\dagger]$, and $\bar{\mathbf{\Omega}}_k = [\mathbf{\Omega}_{k,0}^\dagger\, \mathbf{\Omega}_{k,1}^\dagger \ldots \mathbf{\Omega}_{k,D}^\dagger]^\dagger$.

Assuming that each UE k decodes its message M_k based on the received signal $\mathbf{y}_{k,d}$ by treating the other signals as noise, the following proposition derives a vector of rates $\mathbf{R} \triangleq \{R_k\}_{k\in\mathcal{N}_U}$ that can be supported irrespective of the time offset d. The proposition uses the standard definition for mutual information [10] and is based on assuming the vectors $\bar{\mathbf{v}}_k$ and $\mathbf{x}_{2,k}$ to be circularly symmetric complex Gaussian.

Proposition 1: The following rates are achievable irrespective of the time offset d:

$$R_k = \min_{d\in\mathcal{D}} f_{k,d}(\mathbf{V}, \mathbf{\Sigma}_{\mathbf{x}_2}, \mathbf{\Omega}) \tag{6}$$

where the function $f_{k,d}(\mathbf{V}, \mathbf{\Sigma}_{\mathbf{x}_2}, \mathbf{\Omega})$ is defined as

$$f_{k,d}(\mathbf{V}, \mathbf{\Sigma}_{\mathbf{x}_2}, \mathbf{\Omega}) = I(\mathbf{v}_{k,d}; \mathbf{y}_{k,d}) + I(\mathbf{x}_{2,k}; \mathbf{y}_{k,d}|\bar{\mathbf{v}}_k). \tag{7}$$

The first term $I(\mathbf{v}_{k,d}; \mathbf{y}_{k,d})$ in (7) can be expressed as

$$I(\mathbf{v}_{k,d}; \mathbf{y}_{k,d}) = \log_2 |\mathbf{V}_k| + \log_2 \left|\mathbf{\Sigma}_{\mathbf{y}_{k,d}}\right| - \log_2 |\mathbf{A}_{k,d}| \tag{8}$$

where we defined $\mathbf{V}_k = \mathbb{E}[\mathbf{v}_{k,d}\mathbf{v}_{k,d}^\dagger]$ and the matrices $\mathbf{\Sigma}_{\mathbf{y}_{k,d}}$ and $\mathbf{A}_{k,d}$ are given as

$$\mathbf{\Sigma}_{\mathbf{y}_{k,d}} = \sum_{l\in\mathcal{N}_U} \mathbf{H}_{k,1}\mathbf{V}_l\mathbf{H}_{k,1}^\dagger + \sum_{l\in\mathcal{N}_U} \mathbf{H}_{k,2}\mathbf{\Sigma}_{\mathbf{x}_{2,l}}\mathbf{H}_{k,2}^\dagger + \sum_{l\in\mathcal{N}_U} \mathbf{H}_{k,1}\mathbf{\Omega}_{l,d}\mathbf{H}_{k,2}^\dagger + \sum_{l\in\mathcal{N}_U} \mathbf{H}_{k,2}\mathbf{\Omega}_{l,d}^\dagger\mathbf{H}_{k,1}^\dagger \quad (9)$$

$$\mathbf{A}_{k,d} = \begin{bmatrix} \mathbf{V}_k & \mathbf{V}_k\mathbf{H}_{k,1}^\dagger + \mathbf{\Omega}_{k,d}\mathbf{H}_{k,2}^\dagger \\ \mathbf{H}_{k,1}\mathbf{V}_k + \mathbf{H}_{k,2}\mathbf{\Omega}_{k,d}^\dagger & \mathbf{\Sigma}_{\mathbf{y}_{k,d}} \end{bmatrix} \quad (10)$$

and the second term $I(\mathbf{x}_{2,k};\mathbf{y}_{k,d}|\bar{\mathbf{v}}_k)$ can be written as

$$\begin{aligned} I\left(\mathbf{x}_{2,k};\mathbf{y}_{k,d}|\bar{\mathbf{v}}_k\right) &= f_{k,d,2}\left(\mathbf{V},\mathbf{\Sigma}_{\mathbf{x}_2},\mathbf{\Omega}\right) \quad (11)\\ &= \log_2\left|\mathbf{T}_{k,1}\mathbf{B}_{k,d}\mathbf{T}_{k,1}^\dagger\right| - \log\left|\mathbf{B}_{k,d}\right| \\ &\quad -(D+1)\log\left|\mathbf{V}_k\right| + \log\left|\mathbf{T}_{k,2}\mathbf{B}_{k,d}\mathbf{T}_{k,2}^\dagger\right| \end{aligned}$$

where we defined the matrices

$$\mathbf{B}_{k,d} = \begin{bmatrix} \mathbf{\Sigma}_{\mathbf{x}_{2,k}} & \mathbf{C}_{k,d}^\dagger & \bar{\mathbf{\Omega}}_k^\dagger \\ \mathbf{C}_{k,d} & \mathbf{\Sigma}_{\mathbf{y}_{k,d}} & \mathbf{D}_{k,d}^\dagger \\ \bar{\mathbf{\Omega}}_k & \mathbf{D}_{k,d} & \bar{\mathbf{V}}_k \end{bmatrix} \quad (12)$$

$$\mathbf{C}_{k,d} = \mathbf{H}_{k,1}\mathbf{\Omega}_{k,d} + \mathbf{H}_{k,2}\mathbf{\Sigma}_{\mathbf{x}_{2,k}} \quad (13)$$

$$\mathbf{D}_{k,d} = \left[(\mathbf{H}_{k,2}\mathbf{\Omega}_{k,0}^\dagger)^\dagger \cdots (\mathbf{H}_{k,2}\mathbf{\Omega}_{k,D}^\dagger)^\dagger\right]^\dagger + \mathbf{D}_d^\dagger\mathbf{V}_k\mathbf{H}_{k,1}^\dagger \quad (14)$$

$$\mathbf{T}_{k,1} = \left[\mathbf{0}_{(n_{U,k}+(D+1)n_{R,1})\times n_{R,2}}\ \mathbf{I}_{n_{U,k}+(D+1)n_{R,1}}\right] \quad (15)$$

$$\mathbf{T}_{k,2} = \begin{bmatrix} \mathbf{I}_{n_{R,2}} & \mathbf{0}_{n_{R,2}\times n_{U,k}} & \mathbf{0}_{n_{R,2}\times(D+1)n_{R,1}} \\ \mathbf{0}_{(D+1)n_{R,1}\times n_{R,2}} & \mathbf{0}_{(D+1)n_{R,1}\times n_{U,k}} & \mathbf{I}_{(D+1)n_{R,1}} \end{bmatrix} \quad (16)$$

with $\mathbf{D}_d = [\mathbf{0}_{n_{R,1}\times dn_{T,1}}\ \mathbf{I}_{n_{R,1}}\ \mathbf{0}_{n_{R,1}\times(D-d)n_{R,1}}]$. We also defined the notations $\mathbf{V} \triangleq \{\mathbf{V}_k\}_{k\in\mathcal{N}_U}$, $\mathbf{\Sigma}_{\mathbf{x}_2} \triangleq \{\mathbf{\Sigma}_{\mathbf{x}_{2,k}}\}_{k\in\mathcal{N}_U}$, and $\mathbf{\Omega} = \{\mathbf{\Omega}_{k,d}\}_{k\in\mathcal{N}_U,d\in\mathcal{D}}$.

Proof: It was shown in [8, Th. 2] that the rates R_k in (6) can be achieved with the function $f_{k,d}(\mathbf{V},\mathbf{\Sigma}_{\mathbf{x}_2},\mathbf{\Omega})$ in (7) for a given receiver. The proof is completed by showing that the mutual information quantities $I(\mathbf{v}_{k,d};\mathbf{y}_{k,d})$ and $I(\mathbf{x}_{k,2};\mathbf{y}_{k,d}|\bar{\mathbf{v}}_k)$ are calculated as in (8) and (11), respectively.

To this end, we can express $I(\mathbf{v}_{k,d};\mathbf{y}_{k,d})$ and $I(\mathbf{x}_{k,2};\mathbf{y}_{k,d}|\bar{\mathbf{v}}_k)$ as

$$I\left(\mathbf{v}_{k,d};\mathbf{y}_{k,d}\right) = h(\mathbf{v}_{k,d}) + h\left(\mathbf{y}_{k,d}\right) - h\left(\mathbf{v}_{k,d},\mathbf{y}_{k,d}\right) \quad (17)$$

$$\begin{aligned} I(\mathbf{x}_{k,2};\mathbf{y}_{k,d}|\bar{\mathbf{v}}_k) &= h\left(\mathbf{x}_{2,k}\right) + h\left(\mathbf{y}_{k,d},\bar{\mathbf{v}}_k\right) - h\left(\mathbf{y}_{k,d},\bar{\mathbf{v}}_k,\mathbf{x}_{2,k}\right) \\ &\quad - h\left(\mathbf{x}_{2,k}\right) - h\left(\bar{\mathbf{v}}_k\right) + h\left(\mathbf{x}_{2,k},\bar{\mathbf{v}}_k\right). \quad (18) \end{aligned}$$

Direct calculation of the differential entropy values in (17) and (18) leads to the expressions in (8) and (11), respectively. ■

IV. Problem Definition and Optimization

We aim at optimizing the correlation matrices $\mathbf{V}$, $\mathbf{\Sigma}_{\mathbf{x}_2}$, and $\mathbf{\Omega}$ with the goal of maximizing the worst-case minimum rate $R_{\min} = \min_{k\in\mathcal{N}_U} R_k$ while satisfying the per-RRH power constraints. We can state the problem as

$$\underset{\mathbf{V},\mathbf{\Sigma}_{\mathbf{x}_2},\mathbf{\Omega},R_{\min}}{\text{maximize}} \quad R_{\min} \quad (19a)$$

$$\text{s.t.} \quad R_{\min} \le f_{k,d}\left(\mathbf{V},\mathbf{\Sigma}_{\mathbf{x}_2},\mathbf{\Omega}\right), \text{ for } k\in\mathcal{N}_U,\ d\in\mathcal{D} \quad (19b)$$

$$\sum_{k\in\mathcal{N}_U}\text{tr}(\mathbf{V}_k) \le P_1,\ \sum_{k\in\mathcal{N}_U}\text{tr}\left(\mathbf{\Sigma}_{\mathbf{x}_{2,k}}\right) \le P_2 \quad (19c)$$

$$\mathbf{\Sigma}_{\mathbf{x}}\left(\mathbf{V},\mathbf{\Sigma}_{\mathbf{x}_2},\mathbf{\Omega}\right) \succeq \mathbf{0}, \text{ for } k\in\mathcal{N}_U. \quad (19d)$$

Algorithm 1: CCCP algorithm for problem (19).

1. Initialize the matrices $\mathbf{V}^{(1)}, \mathbf{\Sigma}_{\mathbf{x}_2}^{(1)}, \mathbf{\Omega}^{(1)}$ to arbitrary feasible matrices that satisfy the constraints (19c) and (19d) and set $t = 1$.

2. Update the matrices $\mathbf{V}^{(t+1)}, \mathbf{\Sigma}_{\mathbf{x}_2}^{(t+1)}, \mathbf{\Omega}^{(t+1)}$ as a solution of the following convex problem:

$$\underset{\mathbf{V},\mathbf{\Sigma}_{\mathbf{x}_2},\mathbf{\Omega},R_{\min}}{\text{maximize}} \quad R_{\min} \quad (21a)$$

$$\text{s.t.} \quad R_{\min} \le \tilde{f}_{k,d}\left(\mathbf{V},\mathbf{\Sigma}_{\mathbf{x}_2},\mathbf{\Omega},\mathbf{V}^{(t)},\mathbf{\Sigma}_{\mathbf{x}_2}^{(t)},\mathbf{\Omega}^{(t)}\right)$$

$$\text{for } k\in\mathcal{N}_U,\ d\in\mathcal{D} \quad (21b)$$

$$\sum_{k\in\mathcal{N}_U}\text{tr}\left(\mathbf{V}_k\right) \le P_1,\ \sum_{k\in\mathcal{N}_U}\text{tr}\left(\mathbf{\Sigma}_{\mathbf{x}_{2,k}}\right) \le P_2 \quad (21c)$$

$$\mathbf{\Sigma}_{\mathbf{x}}\left(\mathbf{V},\mathbf{\Sigma}_{\mathbf{x}_2},\mathbf{\Omega}\right) \succeq \mathbf{0}, \text{ for } k\in\mathcal{N}_U. \quad (21d)$$

3. Stop if a convergence criterion is satisfied. Otherwise, set $t \leftarrow t+1$ and go back to Step 2.

A. Optimization

The problem (19) is nonconvex due to the constraints (19b). However, it can be seen that the problem is an instance of the difference-of-convex problems, and hence, we can adopt the concave convex procedure (CCCP)-based approach as in [2] to obtain a sequence of nondecreasing objective values with respect to the number of iterations. The detailed algorithm is described in Algorithm 1, where we defined the functions

$$\begin{aligned} &\tilde{f}_{k,d}\left(\mathbf{V},\mathbf{\Sigma}_{\mathbf{x}_2},\mathbf{\Omega},\mathbf{V}^{(t)},\mathbf{\Sigma}_{\mathbf{x}_2}^{(t)},\mathbf{\Omega}^{(t)}\right) \quad (20)\\ &= \log_2\left|\mathbf{\Sigma}_{\mathbf{y}_{k,d}}\right| + \log_2\left|\mathbf{T}_{k,1}\mathbf{B}_{k,d}\mathbf{T}_{k,1}^\dagger\right| + \log_2\left|\mathbf{T}_{k,2}\mathbf{B}_{k,d}\mathbf{T}_{k,2}^\dagger\right| \\ &\quad - D\cdot\Phi\left(\mathbf{V}_k,\mathbf{V}_k^{(t)}\right) - \Phi\left(\mathbf{A}_{k,d},\mathbf{A}_{k,d}^{(t)}\right) - \Phi\left(\mathbf{B}_{k,d},\mathbf{B}_{k,d}^{(t)}\right) \end{aligned}$$

with the definition $\Phi(\mathbf{A},\mathbf{B}) = \log_2|\mathbf{B}| + \text{tr}(\mathbf{B}^{-1}(\mathbf{A}-\mathbf{B}))/\ln 2$.

The complexity of Algorithm 1 is given by the product of the complexity of solving each convex problem (21) and the number of iterations. The complexity of solving a convex problem is known to be polynomial in the problem size thanks to interior point algorithms [11, Ch. 1 and 11], while the convergence is attained, in our simulation, within a few tens of iterations. We note that the analysis of the convergence rate of general CCCP algorithms is still an open problem to the best of our knowledge.

B. Baseline Schemes

In this subsection, we discuss some baseline schemes.

1) Transmitter Selection: One could avoid the problem of the lack of synchronization by activating only the RRH that

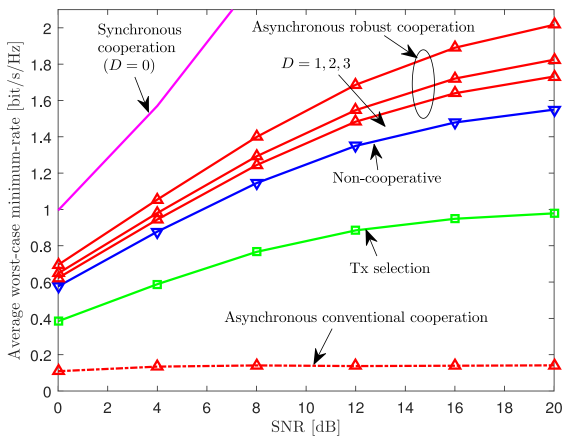

Fig. 2. Average worst-case rate $R_{\min}$ versus the SNR P ($n_{R,i} = n_{U,k} = 1$ and $N_U = 2$).

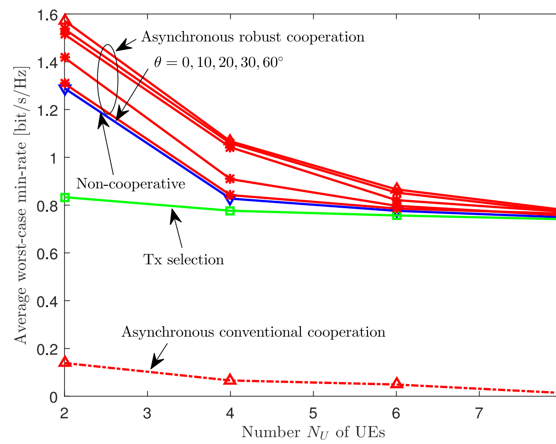

Fig. 3. Average worst-case rate $R_{\min}$ versus the number N_U of UEs ($n_{R,i} = N_U/2$, $n_{U,k} = 1$ and $P = 10$ dB).

supports the largest achievable minimum rate. The performance of this scheme can be obtained by adopting Algorithm 1 with the additional linear constraints $\mathbf{V} = \mathbf{0}$ or $\mathbf{\Sigma}_{\mathbf{x}_2} = \mathbf{0}$, and selecting the solution that yields the best performance.

2) Noncooperative Transmission: A potentially better approach that does not require synchronization is to let the RRHs send independent signals. This approach, referred to as non-cooperative transmission in Section V, includes the transmitter selection scheme as a special case, and the optimization can be addressed by Algorithm 1 with the additional constraints $\mathbf{\Omega} = \mathbf{0}$ (see also [7] for the optimization).

3) Asynchronous Conventional Cooperation: Finally, a conventional approach would be to design the precoding strategy by assuming that the time offset d is zero. This design is obtained from Algorithm 1 by setting $\mathbf{\Omega}_{k,d} = \mathbf{0}$ for $k \in \mathcal{N}_U$ and $d \geq 1$, and removing the constraints (19b) with $d \geq 1$.

We remark that the complexity increment of the proposed robust scheme as compared to the baseline strategies depend on the maximum time offset D, since the scheme requires the optimization of the cross-correlation matrices $\{\mathbf{\Omega}_{k,d}\}_{k\in\mathcal{N}_U, d\in\mathcal{D}}$, which are instead not subject to optimization in the baseline strategies.

V. Numerical Results

In this section, we present some exemplifying numerical results to gauge the potential advantages of the proposed robust scheme as compared to the conventional solutions discussed in Section IV-B. To this end, we consider a symmetric system where the RRHs use the same transmit power $P_1 = P_2 = P$ and the elements of the channel matrices $\mathbf{H}_{k,j}$ are sampled in an independent and identically distributed (i.i.d.) manner from a complex Gaussian distribution with zero mean and unit variance. We used the cvx software [12] to solve the convex problem (21) at each iteration of Algorithm 1, and the maximum number of iterations was set to 50. The worst-case minimum rate was averaged over 100 channel realizations.

Fig. 2 shows the average worst-case rate versus the signal-to-noise ratio (SNR) P for the downlink of a C-RAN with $n_{R,i} = n_{U,k} = 1$ and $N_U = 2$. We set here $\theta = 0$, that is, zero phase offset. For reference, we also show the performance of the synchronous cooperation scheme for which the delay d is perfectly known. It is observed that the proposed robust scheme improves over the noncooperative and transmitter selection schemes with a gain increasing with the SNR. This is in line with the intuition that precoding design becomes more critical in the interference-limited regime of high SNR. However, the performance gain of the proposed robust scheme is reduced as the worst-case time offset D increases. We also emphasize that the conventional nonrobust cooperation scheme that neglects the uncertainty on the time offset performs even worse than the transmitter selection scheme, highlighting the importance of the robust design.

Fig. 3 plots the average worst-case rate versus the number N_U of UEs for the downlink of a C-RAN with $n_{R,i} = N_U/2$, $n_{U,k} = 1$, and $P = 10$ dB. Here, we consider various values of the phase offset θ as indicated in the figure. We emphasize that $n_{R,i} = N_U/2$ is the smallest number of RRH antennas that are able to serve the N_U UEs without creating inter-UE interference in the presence of perfect synchronization. Note that the achievable rates can be easily computed in the presence of a phase offset by using (1) in (7) as done in the proof of Proposition 1. We can see that, although the number $n_{R,i}$ of RRH antennas scales with the number of UEs, the performance of all the schemes is interference limited as long as perfect synchronization is not available. Nevertheless, for a sufficiently small number of UEs, robust cooperation yields significant performance gains, even for phase offsets as high as 20°. However, for larger phase offsets, the observed performance degradation calls for the development of a precoding design that is robust to the phase offset.

VI. Concluding Remarks

Fronthaul limitations constitute one of the key bottlenecks in the implementation of the C-RAN. In this letter, we have considered the aspect of imperfect RRH time synchronization, which may be caused by imperfect clock distribution through the fronthaul network. The proposed robust precoding design was demonstrated to have important advantages, particularly in the high-SNR regime. Among the many interesting open issues, we mention here the design of precoding strategies that are robust to both time and phase offsets, as well as the analysis of models with an arbitrary number of RRHs.

References

[1] O. Simeone, A. Maeder, M. Peng, O. Sahin, and W. Yu, "Cloud radio access network: Virtualizing wireless access for dense heterogeneous systems," *Journ. Commun. Networks*, vol. 18, no. 2, pp. 135–149, Apr. 2016.

[2] S.-H. Park, O. Simeone, O. Sahin, and S. Shamai (Shitz), "Joint precoding and multivariate backhaul compression for the downlink of cloud radio access networks," *IEEE Trans. Signal Process.*, vol. 61, no. 22, pp. 5646–5658, Nov. 2013.

[3] S.-H. Park, O. Simeone, O. Sahin, and S. Shamai (Shitz), "Fronthaul compression for cloud radio access networks: Signal processing advances inspired by network information theory," *IEEE Signal Process. Mag.*, vol. 31, no. 6, pp. 69–79, Nov. 2014.

[4] B. Dai and W. Yu, "Energy efficiency of downlink transmission strategies for cloud radio access networks," *IEEE J. Sel. Areas Commun.*, vol. 34, no. 4, pp. 1037–1050, Apr. 2016.

[5] S. Khalili and O. Simeone, "Uplink HARQ for distributed and cloud RAN via separation of control and data planes," to appear in *IEEE Trans. Veh. Technol.*, available at arXiv:1508.06570.

[6] A. de la Oliva, J. A. Hernandez, D. Larrabeiti, and A. Azcorra, "An overview of the CPRI specification and its application to C-RAN-based LTE scenarios," *IEEE Commun. Mag.*, vol. 54, no. 2, pp. 152–159, Feb. 2016.

[7] M. Xu, D. Guo, and M. L. Honig, "Downlink noncoherent cooperation without transmitter phase alignment," *IEEE Trans. Wireless Commun.*, vol. 12, no. 8, pp. 3920–3931, Aug. 2013.

[8] M. Yemini, A. Somekh-Baruch, and A. Leshem, "On the multiple access channel with asynchronous cognition," available at arXiv:1503.08413.

[9] M. Benammar, P. Piantanida, and S. Shamai (Shitz), "On the compound broadcast channel: Multiple description coding and interference decoding," to appear in *IEEE Trans. Inf. Theory*, available at arXiv:1410.5187.

[10] A. E. Gamal and Y.-H. Kim, *Network Information Theory*. Cambridge, U.K.: Cambridge Univ. Press, 2011.

[11] S. Boyd and L. Vandenberghe, *Convex Optimization*. Cambridge, U.K.: Cambridge Univ. Press, 2004.

[12] M. Grant and S. Boyd, "CVX:Matlab software for disciplined convex programming," ver. 2.0 beta, Sep. 2013. [Online]. Available: http://cvxr.com/cvx